Fish and Shellfish Immunology 124 (2022) 289–299

Contents lists available at ScienceDirect

Fish and Shellfish Immunology

journal homepage: www.elsevier.com/locate/fsi

Molecular delineation, expression profiling, immune response, and anti-apoptotic function of a novel clusterin homolog from big-belly seahorse (*Hippocampus abdominalis*)

H.M.S.M. Wijerathna [a], Kishanthini Nadarajapillai [a], H.M.V. Udayantha [a], T.D.W. Kasthuriarachchi [a], K.A.S.N. Shanaka [a], Hyukjae Kwon [a,b], Qiang Wan [a,b], Jehee Lee [a,b,*]

[a] Department of Marine Life Sciences & Fish Vaccine Research Center, Jeju National University, Jeju, 63243, Republic of Korea
[b] Marine Science Institute, Jeju National University, Jeju, 63333, Republic of Korea

ARTICLE INFO

Keywords:
Hippocampus abdominalis
Clusterin
Oxidative stress
Anti-apoptotic effect
Innate immune responses

ABSTRACT

Clusterin (CLU) is a glycoprotein that contains α- and β-chains. CLU exerts multifunctional activities and plays a role in different cell signaling pathways that are associated with various diseases such as proteotoxic and oxidative stress, as well as cell death and survival. However, its role in marine teleost fish remains unclear. Therefore, the present study was carried out to characterize and investigate the immune responses and anti-apoptotic effects of CLU of the big-belly seahorse (*Hippocampus abdominalis*) (HaCLU) on oxidative stress-induced cell death. The *HaCLU* open reading frame was 1389 bp long and encoded a protein with 462 amino acids, a molecular weight of 51.28 kDa and an isoelectric point of 5.41. *In-silico* results demonstrated that HaCLU has a signal peptide in the 1–29 amino acid region, while the α- and β-chains were in the 34–227 and 228–455 amino acid regions, respectively. Multiple sequence alignment clarified the low homology of the α-chain with other orthologs. The highest HaCLU mRNA expression level was observed in the liver, followed by the heart, spleen, and brain tissues of healthy big-belly seahorses. Further, *HaCLU* mRNA expression level was elevated in the liver in response to different stimuli, including lipopolysaccharides, polyinosinic:polycytidylic acid, *Edwardsiella tarda*, and *Streptococcus iniae*. HaCLU potentiates cell viability and weakens chromatin condensation in the nucleus of FHM cells following H_2O_2-induced oxidative stress and subsequent cell death. HaCLU overexpression resulted in a reduced *Bax/Bcl*-2 mRNA expression ratio. This study revealed the role of HaCLU in immune regulation against pathogenic infections and its anti-apoptotic effects on oxidative stress-induced cell death.

1. Introduction

Clusterin (CLU), also known as apolipoprotein J, is a multifunctional glycoprotein that contains two chains, α- and β-CLU linked by five disulfide bonds [1–3]. This two coiled-coil (CC) domain is important for the interaction of CLU with other proteins to elicit several cellular activities, including stabilizing the Ku70-Bax complex to inhibit mitochondrial apoptosis [3].

CLU was first discovered as a cell-aggregating factor in the ram rete testis fluid of immature rats [4]. Two forms of CLU molecules are ubiquitously expressed in mammals [5], namely CLU precursor forms (approximately 60 kDa) and mature secreted heterodimeric glycoprotein (approximately 75–80 kDa) [5,6]. CLU participates in several physiological and pathological processes, including extracellular chaperone function, lipid transportation, immune modulation, oxidative and proteotoxic stress, cell death, and survival [2,7,8]. A previous study on zebrafish CLU showed that CLU has direct or indirect involvement in neuronal cell death [9], while another study characterized two CLU isoforms, i.e., CLU-1 and CLU-2 in rainbow trout [10]. Although several studies have described the different roles of mammalian CLU, functional studies of its teleost counterparts are obscure.

Accumulating evidence suggests that intracellular CLU is an anti-apoptotic molecule responsible for impairing mitochondrial apoptosis by inhibiting the intrinsic apoptosis pathway through the attenuation of Bax activation in mammals [3,11,12]. Apoptosis is an important biological process for normal cell turnover, proper functioning of the

* Corresponding author. Marine Molecular Genetics Lab, Jeju National University, 102 Jejudaehakno, Jeju, 63243, Republic of Korea.
E-mail address: jehee@jejunu.ac.kr (J. Lee).

https://doi.org/10.1016/j.fsi.2022.04.015
Received 2 January 2022; Received in revised form 11 March 2022; Accepted 11 April 2022
Available online 14 April 2022

immune system, immune system development, chemical-induced cell death, embryonic development, and hormone-dependent atrophy [13]. Furthermore, apoptosis of host cells can be promoted by the pathogen infection induced oxidative stress to suppress the immune system [14]. Moreover, the two types of apoptotic pathways, extrinsic and intrinsic, are clearly defined in previous studies [15,16]. On the one hand, the extrinsic pathway is mediated by the activation of death receptors such as TNFR, Fas, and TRAIL by external environmental influences and leads to the recruitment and activation of initiator caspases (caspases 8 and 10), subsequently leading to the formation and activation of the death-inducing signaling complex (DISC) and caspase 3 [17]. On the other hand, intrinsic apoptosis is mostly initiated by cytochrome *c* release from the mitochondria due to stress factors such as reactive oxygen species (ROS) production and subsequent activation of caspases 9 and 3, inducing cellular apoptosis [17,18]. However, the lack of evidence on the role of teleost CLU in cellular apoptosis and immune response prompted us to investigate the regulatory effect of big-belly seahorse HaCLU on the cellular apoptosis mechanism and immune response against pathogen infections.

Big-belly seahorse (*Hippocampus abdominalis*) is rich in proteins with essential amino acids. They have a high ratio of aromatic or heterocyclic (Pro, His, Phe, and Tyr) and acidic (Asp and Glu) amino acids, which are important in the production of proteins and different products in the aquaculture industry [19,20]. Furthermore, recent studies have indicated that amino acids, unsaturated fatty acids, trace elements, and other functional components in seahorses have medicinal value, particularly in East Asian countries [21–24]. Ryu et al. investigated a novel peptide (SHP-1) from seahorse (*Hippocampus kuda*) hydrolysate for its inhibitory function on collagen release in arthritis [20]. Another study reported that Brassicasterol, a bioactive compound from *Hippocampus abdominalis,* can potentially function as an anti-cancer compound against human prostate cancer [22]. These properties make big-belly seahorse a valuable, highly sought-after marine animal, primarily in the Asian medicinal market [24]. Therefore, customer demand for seahorses is very high not only in Asian countries but also globally, commanding high prices [25,26]. However, captive breeding and rearing of seahorses are challenging because of disease outbreaks caused by pathogens [25]. Thus, to address this issue genetically, research on marine molecular genetics is paramount to improving efficiency for successful seahorse-aquaculture. In this study, we present the first *in silico* analysis and expression pattern, immune response, and anti-apoptotic behaviors of big-belly seahorse HaCLU.

2. Materials and methods

2.1. In-silico analysis of CLU from big-belly seahorse

The full-length *CLU* coding sequence of big-belly seahorse was obtained from a previously established big-belly seahorse transcriptome database. Verification and confirmation of the identified *CLU* were performed using the National Center for Biotechnology Information (NCBI) Basic Local Search Tool (BLAST) [27] and designated as *HaCLU*. The open reading frame and the amino acid sequence of *HaCLU* were predicted using the Unipro UGENE software [28]. Possible domains, motifs, and signal peptides were determined using the Simple Modular Architecture Research Tool (SMART) program [29] and the NCBI conserved domain search tool [30]. The tertiary three-dimensional (3D) structure of HaCLU was predicted using the Iterative Threading ASSEmbly Refinement (I-TASSER) server [31]. Visualization and editing were performed using PyMOL Molecular Graphic System Version 2.5.1 [32]. Multiple sequence analysis and pairwise sequence alignment of HaCLU with other vertebrate orthologs were performed using the Clustal Omega Multiple Sequence alignment tool [33] with the Sequence Manipulation Suite (SMS): Color align conservation tool (https://www.biologicscorp.com/sms2/color_ align_cons.html) and EMBOSS Needle Pairwise sequence alignment tool, respectively [34]. A phylogenetic tree was constructed using the MEGA version 11 software, with 5000 bootstrap replicates, and neighbor-joining method [35].

2.2. Construction of plasmids

Gene-specific PCR primers with appropriate restriction sites (Table 1) were used to construct the full-length *HaCLU* gene from the genomic cDNA of the laboratory big-belly seahorse cDNA library. The gene was cloned into the pcDNA 3.1 (+) vector (Invitrogen, Carlsbad, CA, USA) and pEGFP-N1 (Invitrogen) expression vector to construct the pcDNA 3.1(+)-*HaCLU* and pEGFP-N1-*HaCLU* plasmids, respectively. The cloning was confirmed by sequencing the inserted coding sequence (Macrogen, Republic of Korea).

2.3. Cell culture and gene transfection

Fathead minnow (FHM) cells were cultured and maintained in Leibovitz L-15 medium (Sigma-Aldrich, St. Louis, MO, USA) with 10% heat-inactivated fetal bovine serum (FBS, Gibco-BRL; Life Technologies, Carlsbad, CA, USA) as a supplement and 1% antibiotic-antimycotic (Gibco-BRL; Life Technologies) at 25 °C in an incubator. Thereafter, the constructed plasmids were transfected into FHM cells using the X-tremeGENE™ 9 transfection reagent (Roche Diagnostics GmbH, Penzberg, Germany) according to the manufacturer's protocol.

2.4. Subcellular localization of HaCLU

FHM cells were seeded into a 12-well cell culture plate at a density of 2×10^5 cells/well. After 24 h, cells were transfected with the pEGFP-N1 vector or pEGFP-N1-*HaCLU* plasmid construct. After incubating transfected cells at 25 °C in an incubator for 24 h, the cells were washed with 1 × PBS and fixed with 4% formaldehyde for 10 min. Fixed cells were then stained with 4,6-diamino-2-phenylindole (DAPI) (Invitrogen) for 15 min at 37 °C and washed again with 1 × PBS for observation under a fluorescence microscope at 400 × magnification (Leica DM6000 B; Leica Microsystems, Wetzlar, Germany). The obtained images were processed using Leica Application Suite X version 3.3.

2.5. Experimental animal and tissue isolation

Big-belly seahorses (~8 g average body weight) were bought from the Center of Ornamental Fish Breeding at Jeju Island, Republic of Korea. Fish were transported to the Marine Science Research Institute of Jeju National University, Hamdeok, Jeju, and kept in a 300-L aquarium tank with fresh seawater for one week to acclimatize the fish before the experiments. Fish were fed ad libitum with frozen Mysis shrimp twice per day during the acclimatization period. Water temperature and salinity were maintained at 18 ± 2 °C and 34 ± 0.6‰, respectively. All experimental procedures were performed in accordance with the guidelines provided by the Animal Experiment Ethics Committee of Jeju National University.

To perform the tissue distribution analysis, six fish (three males and three females) were dissected to harvest the skin, kidney, ovary, spleen, blood, heart, brain, intestine, pouch, testis, liver, muscle, gills, and stomach tissues. Blood samples were collected from the verge of the tail by cutting, and hemocytes were separated by centrifugation at 3000×*g* for 10 min at 4 °C. Harvested tissue samples were immediately flash-frozen in liquid nitrogen and stored at −80 °C until further experiments.

2.6. In vivo immune challenge and stimulation

Pre-acclimatized big-belly seahorses (average bodyweight ~3 g) were used in the immune challenge experiment. The fish were divided into five groups, each consisting of 30 individuals. The control group was intraperitoneally injected with 100 μL of PBS. Other groups were challenged intraperitoneally with 100 μL 10^5 CFU/μL of *Streptococcus*

Table 1
Primers used for cloning and qPCR analysis.

Primer name	Sequence (5`-3`)	Application
HaCLU_pcDNA (Forward)	GAGAGAaagcttGCAATGGTGATGATGATGATGATGAAGATGAGGAA (*Hind*III)	Cloning into pcDNA3.1(+)
HaCLU_pcDNA (Reverse)	GAGAGAgaattcCTATTTGGCAACAACAGTGATATCCTTGTAGCG (*Eco*RI)	
HaCLU_pEGFP (Forward)	GAGAGAaagcttATGTTGATGATGATGATGATGAAGATGAGGAA (*Hind*III)	Cloning into pEGFP-N1
HaCLU_pEGFP (Reverse)	GAGAGAggtaccGTTTGGCAACAACAGTGATATCCTTGTAGCG (*Kpn*I)	
HaCLU_qPCR (Forward)	GACGTGGTCATCACCAAACCTTAC	qPCR analysis
HaCLU_qPCR (Reverse)	CCGGAACAATCGACGTGTTCAATC	
Bax_qPCR (Forward)	TGGCACTGTTTCACCTCG	To analyze expression in FHM cells
Bax_qPCR (Reverse)	ATCCTCCTTGCTGTCTGATC	
Bcl-2_qPCR (Forward)	TGGGACTGTTTGCCTTCG	To analyze expression in FHM cells
Bcl-2_qPCR (Reverse)	TCTGCCGCTGCATCTTTT	
EF1α_qPCR (Forward)	GGCTGACTGTGCTGTGCTGAT	qPCR internal reference of FHM cells
EF1α_qPCR (Reverse)	GTGAAAGCCAGGAGGGCATGT	

iniae, 5×10^3 CFU/μL of *Edwardsiella tarda*, 1.25 μg/μL of lipopolysaccharides, from *Escherichia coli* 055:B5 (LPS) (Sigma-Aldrich), and 1.5 μg/μL of polyinosinic: polycytidylic acid (poly I:C). Liver samples were collected from five individuals per group at 0, 3, 6, 12, 24, 48, and 72 h post-injection (p.i.) and kept frozen in liquid nitrogen (−80 °C) for further experiments.

2.7. Quantitative real-time PCR

Total RNA was isolated from FHM cells and big-belly seahorse tissues using the RNAiso Plus kit (Takara Bio Inc, Shiga, Japan). RNA cleaning was performed using an RNeasy spin column (Qiagen, Hilden, Germany). The isolated RNA concentration was quantified using a spectrophotometer at an absorbance of 260 nm (μDrop Plate; Thermo Fisher Scientific, Waltham, MA, USA). Thereafter, cDNA synthesis was performed using the PrimerScript II First Strand cDNA Synthesis Kit (Takara Bio Inc) and quantified by qPCR using TB Green® Premix Ex Taq™ (Tli RNaseH Plus; Takara Bio Inc) in a Thermal Cycler Dice™ Real-Time System III, (Model: TP951; Takara Bio Inc). qPCR primers were designed using the IDT Primer Quest Tool, and the primers are shown in Table 1. The manufacturer's protocols were followed for each step. The transcription level of *HaCLU* was calculated using the Livak $2^{-\Delta\Delta CT}$ method [36].

2.8. MTT assay

FHM cells were seeded at a concentration of 2×10^5 cells/well in a 24-well plate in a cell culture medium for 24 h at 25 °C in an incubator. Subsequently, different concentrations of H_2O_2 (0, 1, 1.5, 2, 3, and 4 mM) were added and incubated at 25 °C for 24 h in the cell culture medium. The MTT assay was performed according to the method described by Kumar et al. with some modifications [37]. Briefly, the medium was removed and replaced with 100 μL serum-free media and 200 μL of 0.5 mg/mL 3-(4,5-dimethylthiazol-2-yl)-2, 5-diphenyltetrazolium bromide (MTT). Thereafter, the plate was covered with aluminum foil and kept at 25 °C in an incubator for 3 h. After incubation in serum-free media, MTT in the wells was replaced with 200 μL dimethyl sulfoxide (DMSO), covered with an aluminum foil, and incubated on a shaker at room temperature (RT) for 30 min. Finally, 50 μL of DMSO from each well was transferred to a 96-well plate to measure absorbance using a Multiskan Sky microplate reader (Thermo Fisher Scientific) at 540 nm. The experiment was performed in triplicate, and the percentage of cell viability was calculated by considering control cells as 100% viable. Suitable concentrations were selected based on the results for future experiments.

To investigate the cell viability percentage of HaCLU-overexpressed FHM cells following treatment with H_2O_2, cells were transfected with pcDNA3.1(+) or pcDNA3.1(+)-*HaCLU* and 20 μL of H_2O_2 in a concentration series (0, 2, 2.5, 3, 3.5, and 4 mM) for 24 h. Afterward, an MTT assay was performed in triplicate as described above to calculate the percentage cell viability using the following equation: cell viability % = $[A_t/A_c] \times 100$, where, A_t represents the mean absorbance value of the test cells and A_c represents the mean absorbance value of the control cells.

2.9. Hoechst assay

Hoechst staining was performed according to a previously described method [38]. Briefly, FHM cells were seeded at a concentration of 3×10^5 cells/well in cell culture medium and incubated at 25 °C for 24 h. Thereafter, cells were transfected with pcDNA 3.1(+) or pcDNA 3.1 (+)-*HaCLU*. Twenty-four hours later, the pcDNA 3.1(+) or pcDNA 3.1 (+)-*HaCLU*-transfected cells were treated with 2 mM H_2O_2 (final concentration) or an equivalent volume of 1 × PBS (control) in existing cell culture medium. After 24 h incubation at 25 °C, apoptotic bodies were observed and counted by staining the cells with 20 μg/mL nuclear-specific Hoechst 33342 dye (Sigma-Aldrich). Nuclei with chromatin condensation were visualized using a fluorescence microscope equipped with a CoolSNAP-Pro color digital camera (Media Cybernetics Inc, Rockville, MD, USA). The apoptotic body index was calculated for each treatment using the following equation: apoptotic body index = (n $[T_b/N_t]$/n$[C_b/N_c]$), where T_b represents the number of apoptotic bodies and N_t represents the number of total nuclei in H_2O_2-treated pcDNA 3.1 (+) or pcDNA 3.1(+)-*HaCLU*-transfected cells or 1 × PBS treated pcDNA 3.1(+)-*HaCLU*-transfected cells, C_b represents the number of apoptotic bodies, and N_c represents the number of total nuclei in 1 × PBS-treated pcDNA3.1(+) transfected cells, while "n" represents the mean values. The minimum number of apoptotic bodies was considered as one in the calculation. The experiment was performed in triplicate.

2.10. Analysis of Bax and Bcl-2 transcriptional level

FHM cells (4×10^5 cells/well) were transfected with pcDNA3.1(+) or pcDNA3.1(+)-*HaCLU* and exposed to 2 mM H_2O_2 in a 12-well cell culture plate; control cells were kept without exposure to H_2O_2. After 24 h incubation with the recommended FHM cell culture conditions, cells were harvested, cDNA was synthesized, and RT-qPCR was performed to analyze Bcl-2-associated X (*Bax*) and B-cell lymphoma 2 (*Bcl-2*) transcription levels using the primers listed in Table 1. The *Bax/Bcl-2* fold-induction ratio was calculated to determine the effect of HaCLU in FHM cells on cellular apoptosis.

2.11. Statistical analysis

All experiments were performed in triplicate, and the results are shown as the mean ± standard deviation. The data were analyzed using Student's *t*-tests and the GraphPad Prism Version 8.0.2 software (GraphPad Software, Inc., San Diego, CA, USA) to determine the differences between the groups. Statistical significance was set at $P < 0.05$.

3. Results

3.1. In silico analysis of HaCLU sequence

The *HaCLU* sequence was extracted from the laboratory pre-constructed big-belly seahorse transcriptome database, and the sequence was submitted to NCBI GenBank (GenBank accession number: OL310706). *HaCLU* was found to contain 1389-bp nucleotides and 462 amino acids. The molecular weight of HaCLU was calculated to be 52.8 kDa, and the theoretical isoelectric point (pI) was found to be 5.41. Furthermore, HaCLU contains an N-terminal signal peptide (1–29 aa), clusterin-β (CLβ) chain (34–227 aa), and a C-terminal clusterin-α (CLα) chain (228–455 aa) (Fig. 1A). The predicted tertiary 3D structure, designed using I-TASSER, showed a similar arrangement with an approximately helical shape (Fig. 1B). Furthermore, the C-score of the predicted structure was indicated as −1.35, in I-TASSER. The C-score ranged from −5 to 2, with a higher C-score indicating higher confidence [31].

Multiple sequence alignment of HaCLU showed highly conserved amino acids with other vertebrate orthologs (Fig. 2). Pairwise comparison of HaCLU (Table 2) with the CLU of *Hippocampus comes* (tiger tail seahorse), which belongs to the same genus, showed the highest identity (97.2%) and similarity (98.9%), followed by that of *Oreochromis* sp. With an identity and similarity of 73.3 and 84.7%, respectively, among the selected orthologs of other vertebrates. However, the CLU of other taxonomies showed an identity lower than 50% with HaCLU. Similarly, phylogenetic tree construction illustrated that HaCLU closely clustered with *Hippocampus comes* in the teleost clade (Fig. 3).

3.2. Subcellular localization of HaCLU

Subcellular localization of HaCLU was observed by transfecting the GFP-tagged pEGFP-N1 plasmid and pEGFP-N1-*HaCLU* construct into FHM cells (Fig. 4). Fluorescence images displayed dispersed green fluorescent-tagged HaCLU throughout the cytoplasm, except the nucleus, which was stained with DAPI (blue color).

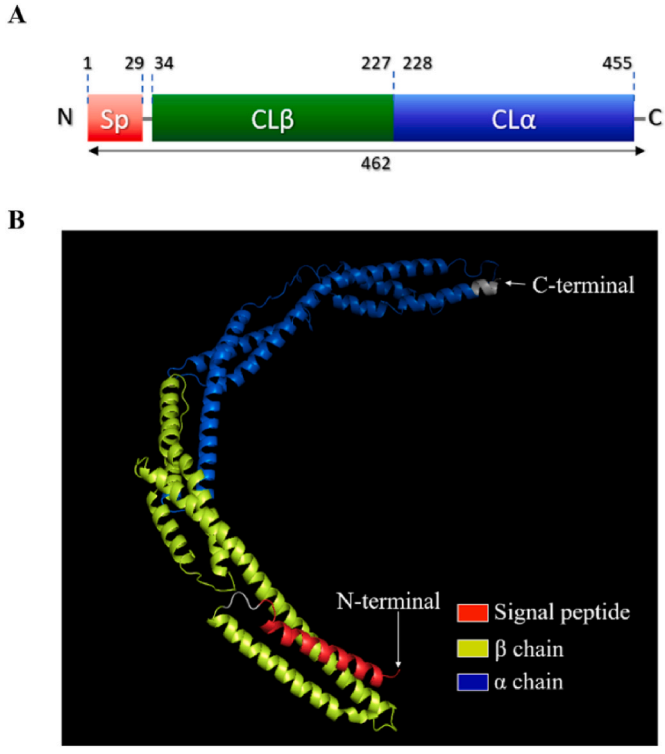

Fig. 1. Domain structure (A) and predicted tertiary 3D structure (B) of HaCLU. The domain structure was predicted by using the SMART embl online tool. The 3D structure was predicted through the I-TASSER Server and edited using the PyMOL software. (Sp, signal peptide; CLβ, β-chain; CLα, α-chain).

3.3. HaCLU mRNA expression pattern in different tissues of big-belly seahorse

RT-qPCR analysis was performed to determine the mRNA expression of *HaCLU* in different big-belly seahorse tissues. As seen in Fig. 5, the highest *HaCLU* mRNA expression level was observed in liver tissue (~44.4 fold), followed by heart (~43.6 fold), spleen (~40.8 fold), and brain (~39.1 fold). However, other tissues showed comparatively lower expression levels, while the intestine had the lowest *HaCLU* expression, which was defined as the basal level.

3.4. Effect of in vivo immune stimulation in big-belly seahorse on temporal HaCLU mRNA expression

To investigate the temporal expression pattern of *HaCLU* in big-belly seahorse following immune stimulation with LPS, poly I:C, *E. tarda* and *S. iniae*, RT-qPCR analysis was performed on the harvested liver tissue at different time points (0, 3, 6, 12, 24, 48, and 72 h) p.i (Fig. 6). Results showed significant induction of *HaCLU* mRNA expression level following LPS challenge at 24 h p.i. Poly I:C challenge shows undulatory modulation of *HaCLU* mRNA expression level with significant induction at 3, 24, and 72 h p.i.; however, the expression level was drastically induced at 24 h p.i. Following *E. tarda* challenge, the expression level increased at 72 h p.i., while *S. iniae* significantly induced the expression level at 24 h p.i., which was later downregulated at 48 h p.i and subsequently upregulated at 72 h p.i.

3.5. Effect of HaCLU on FHM cell survival under H_2O_2-induced oxidative stress

To determine the cytotoxic H_2O_2 dose in FHM cells, cells were treated with increasing concentrations of H_2O_2 (1, 1.5, 2, 3, and 4 mM), and cell viability was observed 24 h post-treatment using the MTT assay. Results indicated that H_2O_2 impaired cell viability with increasing concentration (Fig. 7A); maximum cell death was observed at 4 mM H_2O_2, with 35 ± 1% cell viability. Moreover, the first lowest cell viability lower than 50% was observed at an H_2O_2 concentration of 3 mM (56 ± 1%). However, H_2O_2 concentrations greater than 1.5 mM resulted in significant cell death compared to that in the control cells. Based on the above results, we decided to use a 2–4 mM range of H_2O_2 concentrations for subsequent experiments in this study.

To investigate the effect of HaCLU on H_2O_2-induced oxidative stress and subsequent cell death, pcDNA 3.1(+) or pcDNA 3.1(+)-*HaCLU*-overexpressing FHM cells were treated with increasing concentrations of H_2O_2 (2, 2.5, 3, 3.5, and 4 mM). After a 24-h incubation period, an MTT assay was performed, and the results are illustrated in Fig. 7B. The results revealed that HaCLU-overexpressing FHM cells showed significantly increased levels of cell viability at all H_2O_2 concentrations compared with the pcDNA 3.1(+) vector-transfected FHM cells.

3.6. HaCLU reduces H_2O_2-induced chromatin condensation in the nuclei of apoptotic FHM cells

The ability to reduce chromatin condensation in the nuclei of apoptotic cells during cell death was further determined using Hoechst 33342 staining. As shown in Fig. 8A, HaCLU overexpression in FHM cells reduced the number of apoptotic bodies or condensed chromatin (white arrows in Fig. 8A) compared with the pcDNA 3.1(+) vector-transfected control after treatment with 2 mM H_2O_2. However, cells not treated with H_2O_2 did not show condensed chromatin or apoptotic bodies at all. The apoptotic bodies in each treatment were counted, and the apoptotic body index was calculated (Fig. 8B). The results revealed a significant

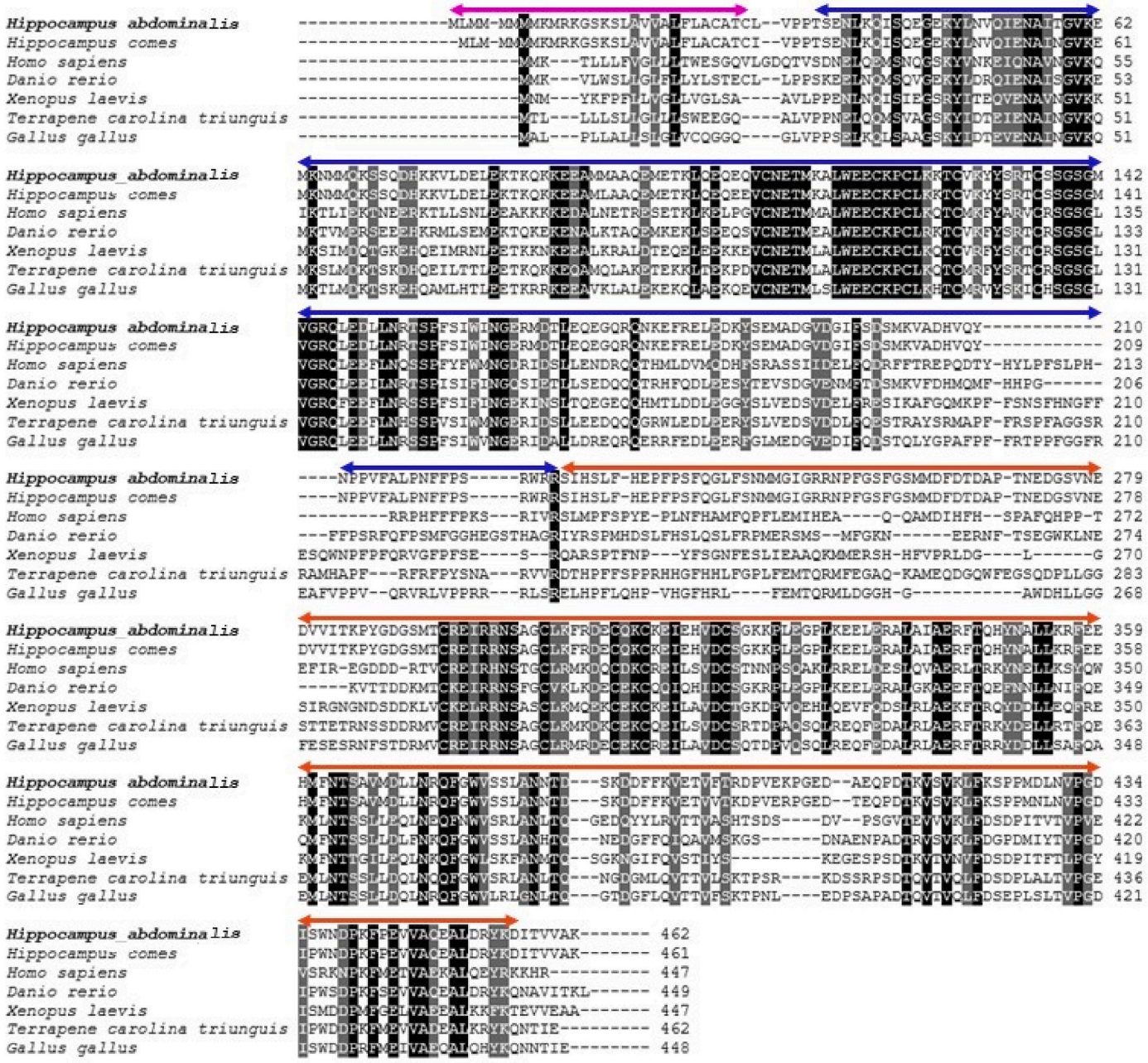

Fig. 2. Multiple sequence alignment of HaCLU (GenBank accession number: OL310706) with its orthologs from different vertebrates. Fully conserved amino acids (aa) are shaded in black and nearly conserved amino acids are shaded in gray. The signal peptide, β chain (CLβ) and α chain (CLα) are indicated by pink, blue, and red lines, respectively.

reduction of apoptotic bodies in HaCLU-overexpressing cells than in the control following H_2O_2 treatment.

3.7. Bax and Bcl-2 transcription after treatment of HaCLU-overexpressing FHM cells with H_2O_2

To analyze the transcription of *Bax* and *Bcl-2* in HaCLU-overexpressing FHM cells after H_2O_2 treatment, RT-qPCR analysis was performed (Fig. 9). Results revealed that HaCLU overexpression reduced the mRNA expression level of *Bax* and increased that of *Bcl-2* (Fig. 9A and B). Furthermore, the *Bax/Bcl-2* fold-induction ratio in HaCLU-overexpressing cells following H_2O_2 treatment was lower than that in the empty vector-transfected cells and cells not exposed to H_2O_2 (Fig. 9C).

4. Discussion

CLU is defined as an “enigmatic” protein, with diverse functions in almost all the fundamental biological processes and various diseases, including cancer [39]. There are various naturally occurring proteoforms of CLU in mammals, including cytosolic, nuclear, and variably glycosylated forms of CLU, which have different functions [2]. Among these functions, the anti-apoptotic effect of CLU is of paramount importance as cell death is an unavoidable and crucial process that occurs in all living organisms [3]. When considering teleost CLU, a previous study investigated the induction of CLU expression following neuronal cell death in zebrafish [9], while another study characterized CLU in rainbow trout and identified two forms of CLU, CLU-1 and CLU-2 [10]. Unfortunately, even though various studies have been done on

Table 2
Pairwise percentage identity and similarity of HaCLU with selected orthologs of other vertebrates.

Species	Accession number	Taxonomy	Identity (%)	Similarity (%)
Hippocampus comes	XP_019726297.1	Fish	97.2	98.9
Oreochromis niloticus	XP_003446372.1	Fish	73.3	84.7
Oreochromis aureus	XP_031584229.1	Fish	73.3	84.7
Gopherus evgoodei	XP_030410953.1	Reptilia	45.7	63.4
Chrysemys picta bellii	XP_005284162.1	Reptilia	45.1	62.7
Gallus gallus	AAD17257.1	Aves	44.7	60.0
Amazona aestiva	KQK80821.1	Aves	43.7	61.2
Numida meleagris	AAW21812.1	Aves	44.2	59.0
Rhinatrema bivittatum	XP_029452092.1	Amphibia	42.8	59.4
Microcaecilia unicolor	XP_030054524.1	Amphibia	41.8	60.0
Geotrypetes seraphini	XP_033794384.1	Amphibia	40.5	59.7
Homo sapiens	AAP88927.1	Mammalia	38.6	57.3
Otolemur garnettii	XP_012663173.1	Mammalia	38.0	55.9

diverse functions of mammalian CLU, studies on functions of teleost CLU are scarce. Hence, the present study sought to elucidate the characteristics, the immune response against different stimulants *in vivo*, and the *in vitro* anti-apoptotic function of HaCLU associated with the immune system.

CLU is an inherently sticky protein; therefore, it has been difficult to produce X-ray crystallographic structures [5]. Hence, we predicted the domain structure and tertiary 3D structure of HaCLU using online tools to gain insight into the characteristics of HaCLU protein. The predicted domain and 3D structure of HaCLU consist of both α- and β-chains structurally similar to their mammalian counterparts [5,40,41]. In teleost, rainbow trout contains two CLU isoforms, CLU-1 and CLU-2, of which CLU-1 is similar to the two CLU chains (α- and β-chains) in mammals [10]. Mammalian CLU is known to comprise a cytoplasmic CLU form (c-CLU) and secreted subunit of CLU (s-CLU), consisting of a signal peptide and, α- and β-chains as the main functional domains [5]. Furthermore, full-length c-CLU consists of α- and β-chains approximately 60 kDa in size, while s-CLU is approximately 40 kDa [6]. Similarly, zebrafish CLU has motifs for the signal peptide and α- and β-chains [9]. In the present study, we found that big-belly seahorse full-length HaCLU is 52.81 kDa with distinct α- and β-chains and an N-terminal signal peptide (Fig. 1). However, the identity and similarity of the HaCLU amino acid sequence in the present study were lower than those of other vertebrate orthologs (Table 2). In addition, the phylogenetic relationship showed that HaCLU clustered together with teleost orthologs (Fig. 3). pEGFP-N1-*HaCLU* overexpression in FHM cells showed that HaCLU localized in the cytoplasm (Fig. 4). Consistent with our observation, a previous study also elucidated that the anti-apoptotic form of CLU localized in the cytoplasm in most primary and metastatic breast

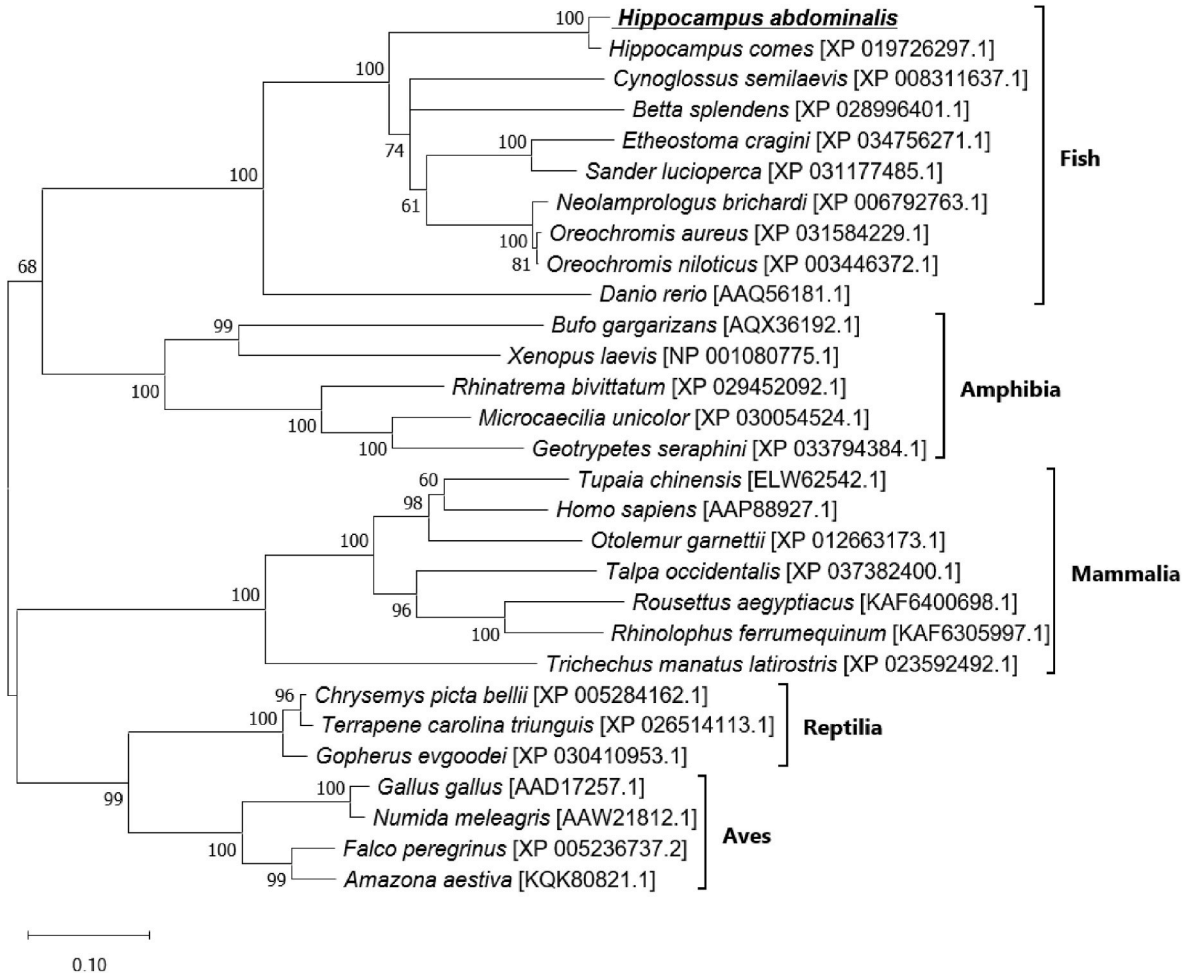

Fig. 3. Phylogenetic relationship of HaCLU (GenBank accession number: OL310706) with orthologs of other vertebrates including Fish, Amphibia, Mammalia, Reptilia, and Aves. *H. abdominalis* is clustered with the teleost clade and shares the same root with *H. comes* but in different branches. The Neighbor-joining method was used, and bootstrap values are shown at nodes of the branches based on 5000 replicates.

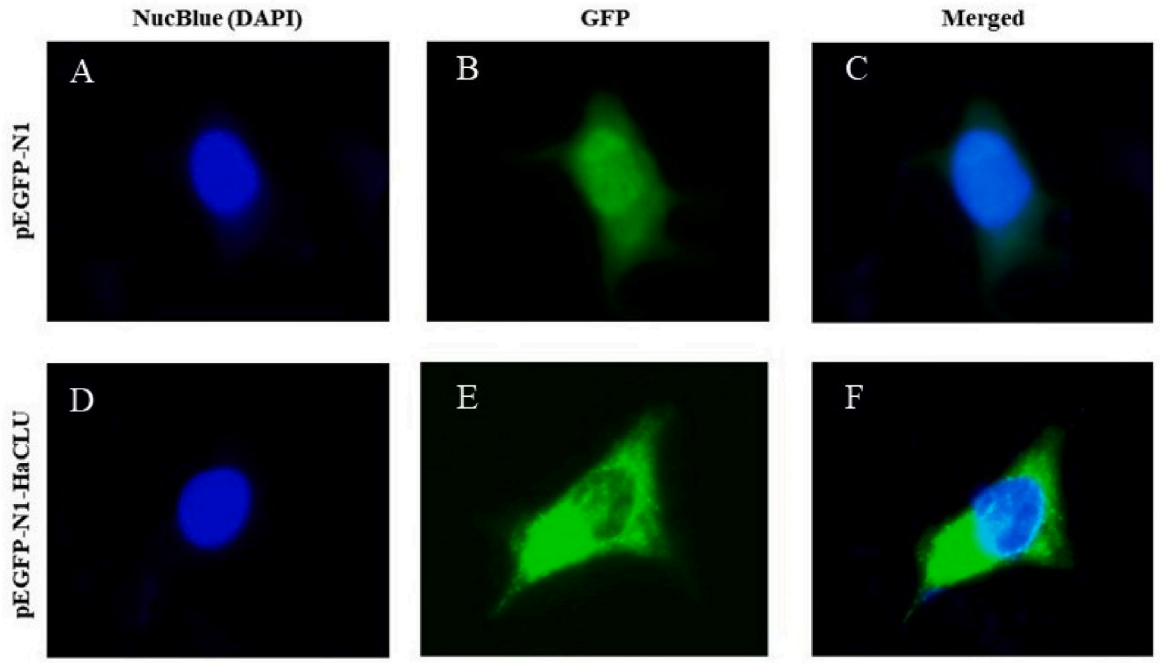

Fig. 4. Subcellular localization of HaCLU in FHM cells. FHM cells were transfected with pEGFP-N1 (A, B, and C) or pEGFP-N1-*HaCLU* (D, E, and F) and incubated for 24 h at 25 °C. Incubated cells were fixed with 3% formaldehyde and the nucleus was stained with DAPI. Images were taken using a fluorescence microscope. pEGFP-N1 or pEGFP-N1-*HaCLU* expression is indicated in green; the nucleus was stained blue, and merged results show the nucleus and fluorescence expression of pEGFP-N1 or pEGFP-N1-*HaCLU* together in the same cell.

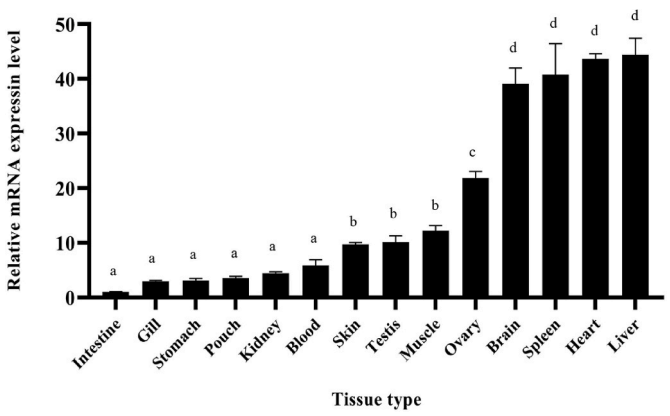

Fig. 5. Relative mRNA expression analysis of *HaCLU* in different tissues of healthy big-belly seahorse. Data are presented relative to the transcript level of the intestine. The liver, heart, spleen, and brain show relatively higher *HaCLU* expression levels, while the liver shows the highest expression relative to the *HaCLU* transcription level of the intestine. Data are presented as the mean values of relative mRNA expression level ± standard deviation (SD) ($n = 3$).

carcinomas, enhancing cancer cell survival [42].

We investigated the tissue distribution of *HaCLU* in different tissues and found higher transcriptional levels of *HaCLU* in the brain, spleen, heart, and liver of healthy big-belly seahorses. The highest *HaCLU* expression was observed in the liver tissue (Fig. 5). Consistent with our result, a previous study also reported that CLU-1 was highly expressed in the liver tissue of rainbow trout [10]. Evidence suggests that CLU is an immune preconditioning regulator in different types of inflammatory diseases in mammals, such as steatohepatitis and subsequent hepatocarcinogenesis in the liver [43,44]. Moreover, Li et al. described the use of the CLU expression patterns in liver tissues as a biomarker for diagnosing hepatocellular carcinoma [44]. In addition, the liver is an immunologically and anatomically unique site that is rich in natural killer and natural killer T cells, which are essential for the innate immune response against pathogen infections [45]. Moreover, the liver plays a major regulatory role during inflammation [46]. When considering our results and previous studies, we were encouraged to analyze the changes in CLU expression in the liver tissue of big-belly seahorses as a means of investigating the immune response of HaCLU against different pathogens and pathogen mimics, including LPS, Poly I:C, *E. tarda* and *S. iniae* (Fig. 6). As expected, we found that both gram-negative (*E. tarda*) and positive (*S. iniae*) bacteria increased *HaCLU* expression in the liver tissue of big-belly seahorse in a time-dependent manner. Similarly, poly I:C, a double-stranded RNA virus mimic, induce *HaCLU* expression in big-belly seahorse liver tissue, providing insight into the potential role of CLU in innate immune function against viral infections. However, evaluating the different expression patterns of immune stimulants at various time points should provide evidence for the different mechanisms of each stimulant in activating HaCLU.

Complex interactions between pathogens and cellular host proteins induce host cell apoptosis under ROS-induced oxidative stress [47]. Previous studies have suggested that c-CLU has anti-apoptotic properties which are important in human cancer therapy [48–50]. Therefore, we sought to determine whether HaCLU had an anti-apoptotic effect against apoptosis stimulants based on the HaCLU, structural analysis and immune challenge results and the accumulated evidence on the anti-apoptotic function of mammalian c-CLU. Apoptosis can occur due to H_2O_2-induced oxidative stress. A previous study indicated that inflammatory and vascular cells could cause oxidative stress by producing H_2O_2, subsequently inducing reactive oxygen species (ROS) such as $O_2^{\bullet-}$ through endothelial nitric oxide synthase (NOS) and nicotinamide adenine dinucleotide phosphate (NADPH) oxidase, contributing to endothelial dysfunction [51]. In the present study, we used FHM cells, an epithelial cell line of fathead minnow, to study the ROS-induced anti-apoptotic function of HaCLU. First, we determined the effective concentration of H_2O_2 required to induce apoptosis in FHM cells and found significant cell death in FHM cells following treatment with H_2O_2 at concentrations higher than 1.5 mM (Fig. 7A). Similarly, in a previous study that investigated the oxidative stress in fish cell lines,

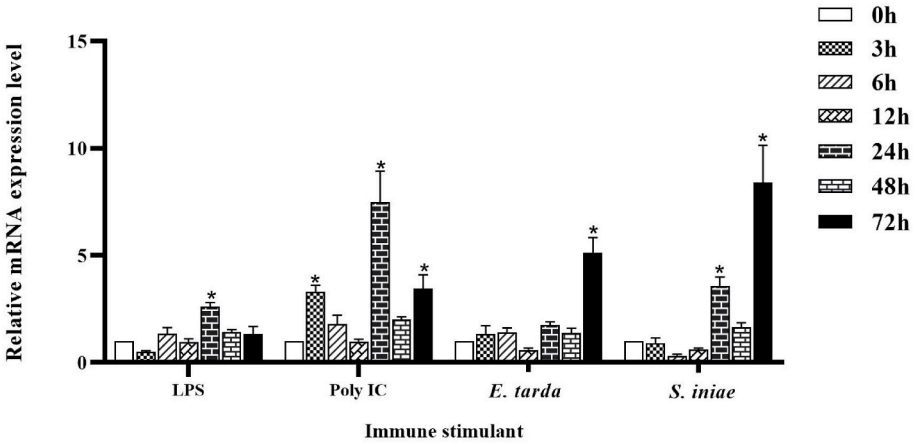

Fig. 6. The relative transcription level of *HaCLU* in the liver of big-belly seahorse after 0, 3, 6, 12, 24, 48, and 72 h following LPS, poly I:C, *E. tarda,* and *S. iniae* challenge. RT-qPCR was performed on liver tissue to quantify the mRNA expression level of *HaCLU* after the challenge, and the fold expressions were normalized to the untreated (at 0 h) and PBS controls. Data are expressed as mean relative mRNA expression level ± SD ($n = 3$). Statistical significances ($p < 0.05$) between control and experimental groups were calculated using Student's *t*-test and indicated by an asterisk (*).

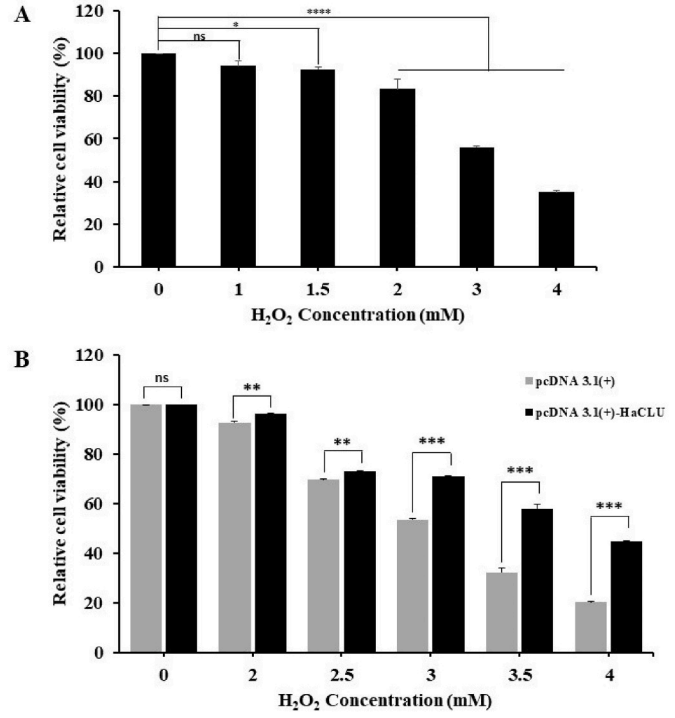

Fig. 7. FHM cell percentage viability at different H_2O_2 concentrations (A). MTT assay was performed 24-h treatments with H_2O_2 at 0-, 1-,1.5-, 2-, 3-, 4- mM concentrations. Thereafter, the best concentration range of H_2O_2 was selected to analyze the percentage cell viability of FHM cells transfected with pcDNA3.1 (+) or pcDNA3.1 (+)-*HaCLU* (B). Transfected FHM cells were treated with 0, 2, 2.5, 3, 3.5, 4 mM of H_2O_2, and cell viability was assessed using an MTT assay. Data are presented as the mean values of percentage cell viability ± SD ($n = 3$). Statistically significances between treatments were compared with the control (0 mM) using Student's *t*-test (ns, $p > 0.05$; *, $p \leq 0.05$; **, $p \leq 0.01$; ***, $p \leq 0.001$; ****, $p \leq 0.0001$).

H_2O_2-induced oxidative stress and cytotoxicity were observed in FHM cells at concentrations higher than 1.5 mM of H_2O_2 [52]. Based on the above findings, the MTT assay was performed using selected H_2O_2 concentrations. Results implied that HaCLU could attenuate H_2O_2-induced apoptotic cell death in FHM cells (Fig. 7B).

The apoptotic process is characterized by a reduction in DNA content and morphological changes such as nuclear condensation [53]. The Hoechst assay is a well-recognized method used to identify apoptotic bodies during cell death and chromatin condensation [53]. Considering this, our Hoechst assay showed a profound effect of HaCLU in reducing the number of apoptotic bodies in H_2O_2-induced apoptotic in HaCLU-overexpressing FHM cells (Fig. 8A and B). Similar evidence was obtained in the Hoechst experimental results of a previous study regarding the anti-apoptotic effect of CLU [12].

To confirm our findings, we investigated the *Bax, Bcl-2*, and *Bax/Bcl-2* expression ratios (Fig. 9). Accumulating evidence suggests that CLU is recognized as an anti-apoptotic molecule in mammals [54–56]. A previous study showed that CLU interferes with *Bax* activation by interacting with conformation-altered Bax, followed by attenuation of Bax oligomerization and subsequent release of cytochrome *c* from mitochondria to continue the intrinsic apoptotic pathway [6]. Oxidative stress can activate the intrinsic apoptotic pathway, which mainly continues through the mitochondria by suppressing the Bcl-2 anti-apoptotic molecule and activating the Bax pro-apoptotic protein [57]. Activated Bax then recruits to the outer membrane of the mitochondria and triggers cytochrome *c* release from the intermembrane space of the mitochondria to the cytosol to induce the formation of the apoptosome and subsequent activation of caspase-3 to continue apoptotic cell death [58]. Hence, the ratio of *Bax* and *Bcl-2* is pivotal in determining the activation of apoptotic events. Regarding the anti-apoptotic activity of CLU, a previous investigation revealed that CLU attenuates cytochrome *c* release by impairing Bax activation and recovering the *Bcl-2/Bax* ratio relative to a control, showing a decreased *Bcl-2/Bax* mRNA expression ratio following treatment with H_2O_2 [12]. Our findings are consistent with the observations of the aforementioned study. Moreover, the α-chain of CLU strongly interacts with Bax, while the β-chain does not [6].

Taken together, the above evidence suggests that HaCLU has the potential to influence the immune regulation process against pathogen infections and function as an anti-apoptotic protein in H_2O_2-induced apoptotic cell death through mechanisms likely similar to those of mammalian CLU.

5. Conclusion

In this study, we determined that the HaCLU amino acid sequence has less identity and similarity with the orthologs of other vertebrates, except fish. However, the predicted domain structure of the full-length *HaCLU* is similar to that of mammalian CLU and mainly consists of a signal peptide and α- and β-chains and is a cytoplasmic form of CLU. *HaCLU* was highly expressed in the liver of big-belly seahorse, as well as in the brain, spleen, and heart, *HaCLU* was also significantly expressed. We further revealed that *HaCLU* might be involved in innate immune activity against LPS, poly I:C, *E. tarda* (gram-negative), and *S. iniae* (gram-positive). Moreover, HaCLU has an anti-apoptotic function, suppressing the H_2O_2-induced oxidative stress and subsequent cell death.

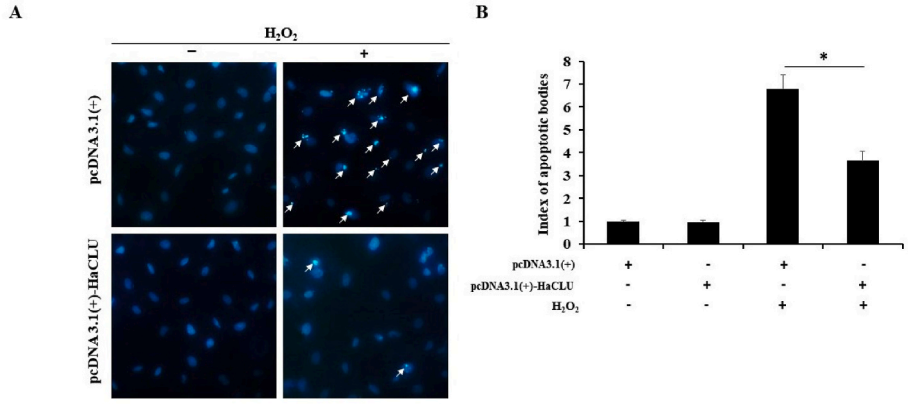

Fig. 8. Effect of HaCLU on chromatin condensation following H_2O_2-induced apoptotic cell death in FHM cells. FHM cells were transfected with pcDNA3.1(+) or pcDNA3.1(+)-*HaCLU* and apoptosis was induced after 24 h incubation at 25 °C using 2 mM H_2O_2. A Hoechst 33342 assay was performed after 24 h incubation, and chromatin condensation was visualized using a fluorescence microscope (A). The apoptotic body index was calculated as the number of apoptotic bodies relative to the total number of cells (B). Arrowheads indicate chromatin condensation. Data are expressed as a mean index of apoptotic bodies ± SD ($n = 3$). Statistical significances between pcDNA3.1 (+) and pcDNA3.1(+)-*HaCLU* transfected cells were determined using Student's *t*-test and indicated by an asterisk (*, $p \leq 0.05$).

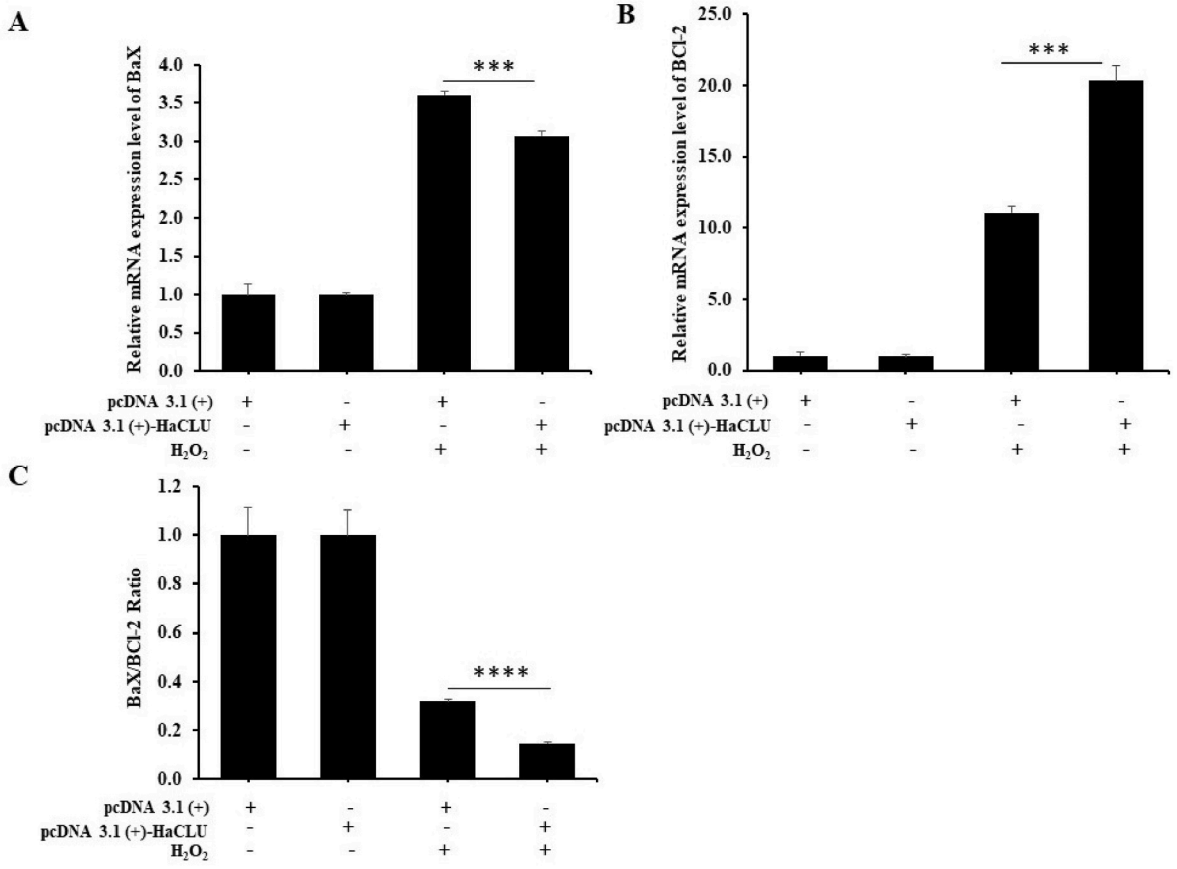

Fig. 9. The relative mRNA expression of *Bax* and *Bcl-2* in HaCLU-overexpressing FHM cells treated with H_2O_2 (A and B) and the ratio of *Bax/BCL-2* expression levels (C). pcDNA3.1(+) or pcDNA3.1(+)-*HaCLU*-over expressing FHM cells were treated with 2 mM of H_2O_2 for 24 h, and RT-qPCR analysis was performed to determine the mRNA expression levels of *Bax* and *Bcl-2*. Data are expressed as mean relative mRNA expression level or ratio ± SD ($n = 3$). Statistical significances between pcDNA3.1(+) and pcDNA3.1(+)-*HaCLU* -transfected cells following H_2O_2 treatment were determined using Student's *t*-test and indicated by an asterisk (***, $p \leq 0.001$; ****, $p \leq 0.0001$).

CRediT authorship contribution statement

H.M.S.M. Wijerathna: Conceptualization, Methodology, Investigation, Formal analysis, Writing – original draft. **Kishanthini Nadarajapillai:** Methodology, Investigation, Writing – review & editing. **H.M. V. Udayantha:** Methodology, Investigation. **T.D.W. Kasthuriarachchi:** Methodology, Investigation. **K.A.S.N. Shanaka:** Writing – review & editing. **Hyukjae Kwon:** Methodology, Investigation. **Qiang Wan:** Methodology, Investigation. **Jehee Lee:** Resources, Supervision, Writing – review & editing, Project administration, Funding acquisition.

Acknowledgments

This research was a part of the project titled 'Fish Vaccine Research Center,' funded by the Ministry of Oceans and Fisheries, Korea, and was supported by the Basic Science Research Program through the National Research Foundation of Korea (NRF) funded by the Ministry of Education (2019R1A6A1A03033553).

References

[1] B. Shannan, M. Seifert, K. Leskov, J. Willis, D. Boothman, W. Tilgen, J. Reichrath, Challenge and promise: roles for clusterin in pathogenesis, progression and therapy of cancer, Cell Death Differ. 13 (2006) 12–19, https://doi.org/10.1038/sj.cdd.4401779.

[2] S.R. Matukumalli, R. Tangirala, C.M. Rao, Clusterin: full-length protein and one of its chains show opposing effects on cellular lipid accumulation, Sci. Rep. 7 (2017) 41235, https://doi.org/10.1038/srep41235.

[3] N. Kim, J.C. Yoo, J.Y. Han, E.M. Hwang, Y.S. Kim, E.Y. Jeong, C.-H. Sun, G.-S. Yi, G.S. Roh, H.J. Kim, S.S. Kang, G.J. Cho, J.-Y. Park, W.S. Choi, Human nuclear clusterin mediates apoptosis by interacting with Bcl-XL through C-terminal coiled coil domain, J. Cell. Physiol. 227 (2012) 1157–1167, https://doi.org/10.1002/jcp.22836.

[4] I.B. Fritz, K. Burdzy, B. Sétchell, O. Blaschuk, Ram rete testis fluid contains a protein (clusterin) which influences cell-cell interactions in Vitro1, Biol. Reprod. 28 (1983) 1173–1188, https://doi.org/10.1095/biolreprod28.5.1173.

[5] S. Jones, Clusterin, Int. J. Biochem. Cell Biol. 34 (2002) 427–431, https://doi.org/10.1016/S1357-2725(01)00155-8.

[6] H. Zhang, J.K. Kim, C.A. Edwards, Z. Xu, R. Taichman, C.-Y. Wang, Clusterin inhibits apoptosis by interacting with activated Bax, Nat. Cell Biol. 7 (2005) 909–915, https://doi.org/10.1038/ncb1291.

[7] P. Rohne, H. Prochnow, S. Wolf, B. Renner, C. Koch-Brandt, The chaperone activity of clusterin is dependent on glycosylation and redox environment, Cell. Physiol. Biochem. 34 (2014) 1626–1639, https://doi.org/10.1159/000366365.

[8] E.M. Foster, A. Dangla-Valls, S. Lovestone, E.M. Ribe, N.J. Buckley, Clusterin in alzheimer's disease: mechanisms, genetics, and lessons from other pathologies, Front. Neurosci. 13 (2019) 164, https://doi.org/10.3389/fnins.2019.00164.

[9] Y.-M. Jeong, T.-E. Jin, J.-H. Choi, M.-S. Lee, H.-T. Kim, K.-S. Hwang, D.-S. Park, H.-W. Oh, J.-K. Choi, V. Korzh, M. Schachner, K.-H. You, C.-H. Kim, Induction of clusterin expression by neuronal cell death in zebrafish, J. Genet. Genom. 41 (2014) 583–589, https://doi.org/10.1016/j.jgg.2014.08.007.

[10] A. Londou, A. Mikrou, I.K. Zarkadis, Cloning and characterization of two clusterin isoforms in rainbow trout, Mol. Immunol. 45 (2008) 470–478, https://doi.org/10.1016/j.molimm.2007.05.027.

[11] I.P. Trougakos, M. Lourda, M.H. Antonelou, D. Kletsas, V.G. Gorgoulis, I. S. Papassideri, Y. Zou, L.H. Margaritis, D.A. Boothman, E.S. Gonos, Intracellular clusterin inhibits mitochondrial apoptosis by suppressing p53-activating stress signals and stabilizing the cytosolic Ku70-Bax protein complex, Clin. Cancer Res. 15 (2009) 48–59, https://doi.org/10.1158/1078-0432.CCR-08-1805.

[12] H.-O. Jun, D. Kim, S.-W. Lee, H.S. Lee, J.H. Seo, J.H. Kim, J.H. Kim, Y.S. Yu, B. H. Min, K.-W. Kim, Clusterin protects H9c2 cardiomyocytes from oxidative stress-induced apoptosis via Akt/GSK-3β signaling pathway, Exp. Mol. Med. 43 (2011) 53, https://doi.org/10.3858/emm.2011.43.1.006.

[13] S. Elmore, Apoptosis: a review of programmed cell death, Toxicol. Pathol. 35 (2007) 495–516, https://doi.org/10.1080/01926230701320337.

[14] K.A. Kim, J.Y. Kim, Y.A. Lee, K.-J. Song, D. Min, M.H. Shin, NOX1 participates in ROS-dependent cell death of colon epithelial Caco2 cells induced by Entamoeba histolytica, Microb. Infect. 13 (2011) 1052–1061, https://doi.org/10.1016/j.micinf.2011.06.001.

[15] L. Duprez, E. Wirawan, T.V. Berghe, P. Vandenabeele, Major cell death pathways at a glance, Microb. Infect. 11 (2009) 1050–1062, https://doi.org/10.1016/j.micinf.2009.08.013.

[16] M.R. Sprick, H. Walczak, The interplay between the Bcl-2 family and death receptor-mediated apoptosis, Biochim. Biophys. Acta Mol. Cell Res. 1644 (2004) 125–132, https://doi.org/10.1016/j.bbamcr.2003.11.002.

[17] L. Portt, G. Norman, C. Clapp, M. Greenwood, M.T. Greenwood, Anti-apoptosis and cell survival: a review, Biochim. Biophys. Acta Mol. Cell Res. 1813 (2011) 238–259, https://doi.org/10.1016/j.bbamcr.2010.10.010.

[18] J.E. Rager, The role of apoptosis-associated pathways as responders to contaminants and in disease progression, in: Systems Biology in Toxicology and Environmental Health, Elsevier, 2015, pp. 187–205, https://doi.org/10.1016/B978-0-12-801564-3.00008-0.

[19] Z. Guo, D. Lin, J. Guo, Y. Zhang, B. Zheng, In vitro antioxidant activity and in vivo anti-fatigue effect of sea horse (*Hippocampus*) peptides, Molecules 22 (2017) 482, https://doi.org/10.3390/molecules22030482.

[20] B. Ryu, Z.-J. Qian, S.-K. Kim, SHP-1, a novel peptide isolated from seahorse inhibits collagen release through the suppression of collagenases 1 and 3, nitric oxide products regulated by NF-κB/p38 kinase, Peptides 31 (2010) 79–87, https://doi.org/10.1016/j.peptides.2009.10.019.

[21] N. Kang, S.-Y. Kim, S. Rho, J.-Y. Ko, Y.-J. Jeon, Anti-fatigue activity of a mixture of seahorse (*Hippocampus abdominalis*) hydrolysate and red ginseng, Fish. Aquat. Sci. 20 (2017) 3, https://doi.org/10.1186/s41240-017-0048-x.

[22] Y. Xu, S. Ryu, Y.-K. Lee, H.-J. Lee, Brassicasterol from edible aquacultural *Hippocampus abdominalis* exerts an anti-cancer effect by dual-targeting AKT and AR signaling in prostate cancer, Biomedicines 8 (2020) 370, https://doi.org/10.3390/biomedicines8090370.

[23] Y. Oh, C.-B. Ahn, N.Y. Yoon, K.H. Nam, Y.-K. Kim, J.-Y. Je, Protective effect of enzymatic hydrolysates from seahorse (*Hippocampus abdominalis*) against H2O2-mediated human umbilical vein endothelial cell injury, Biomed. Pharmacother. 108 (2018) 103–110, https://doi.org/10.1016/j.biopha.2018.08.143.

[24] C.M.C. Woods, Improving initial survival in cultured seahorses, *Hippocampus abdominalis* leeson, 1827 (Teleostei: Syngnathidae), Aquaculture 190 (2000) 377–388, https://doi.org/10.1016/S0044-8486(00)00408-7.

[25] V. LePage, J. Young, C.J. Dutton, G. Crawshaw, J.A. Paré, M. Kummrow, D. J. McLelland, P. Huber, K. Young, S. Russell, L. Al-Hussinee, J.S. Lumsden, Diseases of captive yellow seahorse *Hippocampus kuda Bleeker*, pot-bellied seahorse *Hippocampus abdominalis* Lesson and weedy seadragon *Phyllopteryx taeniolatus* (Lacépède), J. Fish. Dis. 38 (2015) 439–450, https://doi.org/10.1111/jfd.12254.

[26] K.M. Martin-Smith, A.C.J. Vincent, Exploitation and trade of Australian seahorses, pipehorses, sea dragons and pipefishes (Family Syngnathidae), Oryx 40 (2006) 141–151, https://doi.org/10.1017/S003060530600010X.

[27] S. McGinnis, T.L. Madden, BLAST: at the core of a powerful and diverse set of sequence analysis tools, Nucleic Acids Res. 32 (2004) W20–W25, https://doi.org/10.1093/nar/gkh435.

[28] K. Okonechnikov, O. Golosova, M. Fursov, Unipro UGENE: a unified bioinformatics toolkit, Bioinformatics 28 (2012) 1166–1167, https://doi.org/10.1093/bioinformatics/bts091.

[29] J. Schultz, F. Milpetz, P. Bork, C.P. Ponting, SMART, a simple modular architecture research tool: identification of signaling domains, Proc. Natl. Acad. Sci. Unit. States Am. 95 (1998) 5857–5864, https://doi.org/10.1073/pnas.95.11.5857.

[30] A. Marchler-Bauer, M.K. Derbyshire, N.R. Gonzales, S. Lu, F. Chitsaz, L.Y. Geer, R. C. Geer, J. He, M. Gwadz, D.I. Hurwitz, C.J. Lanczycki, F. Lu, G.H. Marchler, J. S. Song, N. Thanki, Z. Wang, R.A. Yamashita, D. Zhang, C. Zheng, S.H. Bryant, CDD: NCBI's conserved domain database, Nucleic Acids Res. 43 (2015) D222–D226, https://doi.org/10.1093/nar/gku1221.

[31] Y. Zhang, I-TASSER server for protein 3D structure prediction, BMC Bioinf. 9 (2008) 40, https://doi.org/10.1186/1471-2105-9-40.

[32] W. DeLano, Pymol: an open-source molecular graphics tool, CCP4 Newsl. Protein Crystallogr. (2002) 700.

[33] F. Sievers, D.G. Higgins, The clustal Omega multiple alignment package, in: K. Katoh (Ed.), Multiple Sequence Alignment, Springer US, New York, NY, 2021, pp. 3–16, https://doi.org/10.1007/978-1-0716-1036-7_1.

[34] P. Rice, I. Longden, A. Bleasby, EMBOSS: the European molecular biology open software suite, Trends Genet. 16 (2000) 276–277, https://doi.org/10.1016/S0168-9525(00)02024-2.

[35] K. Tamura, G. Stecher, S. Kumar, MEGA11: molecular evolutionary genetics analysis version 11, Mol. Biol. Evol. 38 (2021) 3022–3027, https://doi.org/10.1093/molbev/msab120.

[36] K.J. Livak, T.D. Schmittgen, Analysis of relative gene expression data using real-time quantitative PCR and the 2−ΔΔCT method, Methods 25 (2001) 402–408, https://doi.org/10.1006/meth.2001.1262.

[37] P. Kumar, A. Nagarajan, P.D. Uchil, Analysis of cell viability by the MTT assay, Cold Spring Harb. Protoc. 2018 (2018), 095505, https://doi.org/10.1101/pdb.prot095505.

[38] X. Han, K.A. Kang, M.J. Piao, A.X. Zhen, Y.J. Hyun, H.M. Kim, Y.S. Ryu, J.W. Hyun, Shikonin exerts cytotoxic effects in human colon cancers by inducing apoptotic cell death via the endoplasmic reticulum and mitochondria-mediated pathways, Biomol. Therapeut. 27 (2019) 41–47, https://doi.org/10.4062/biomolther.2018.047.

[39] F. Rizzi, M. Coletta, S. Bettuzzi, Chapter 2 clusterin (CLU), in: Advances in Cancer Research, Elsevier, 2009, pp. 9–23, https://doi.org/10.1016/S0065-230X(09)04002-0.

[40] M.E. Fini, S. Jeong, M.R. Wilson, Therapeutic potential of the molecular chaperone and matrix metalloproteinase inhibitor clusterin for dry eye, IJMS 22 (2020) 116, https://doi.org/10.3390/ijms22010116.

[41] P. Wong, T. Ulyanova, D.T. Organisciak, S. Bennett, J. Lakins, J.M. Arnold, R. K. Kutty, M. Tenniswood, T. vanVeen, R.M. Darrow, G. Chader, Expression of multiple forms of clusterin during light-induced retinal degeneration, Curr. Eye Res. 23 (2001) 157–165, https://doi.org/10.1076/ceyr.23.3.157.5463.

[42] M. Redondo, E. Villar, J. Torres-Muñoz, T. Tellez, M. Morell, C.K. Petito, Overexpression of clusterin in human breast carcinoma, Am. J. Pathol. 157 (2000) 393–399, https://doi.org/10.1016/S0002-9440(10)64552-X.

[43] M. Yao, M. Fang, W. Zheng, Z. Dong, D. Yao, Role of secretory clusterin in hepatocarcinogenesis, Transl. Gastroenterol. Hepatol. 3 (2018) 48, https://doi.org/10.21037/tgh.2018.07.13.

[44] Y. Li, F. Liu, W. Zhou, S. Zhang, P. Chu, F. Lin, H.L. Wang, Diagnostic value of clusterin immunostaining in hepatocellular carcinoma, Diagn. Pathol. 15 (2020) 127, https://doi.org/10.1186/s13000-020-01041-8.

[45] V. Racanelli, B. Rehermann, The liver as an immunological organ, Hepatology 43 (2006) S54–S62, https://doi.org/10.1002/hep.21060.

[46] M.W. Robinson, C. Harmon, C. O'Farrelly, Liver immunology and its role in inflammation and homeostasis, Cell. Mol. Immunol. 13 (2016) 267–276, https://doi.org/10.1038/cmi.2016.3.

[47] S.E. Hasnain, R. Begum, K.V.A. Ramaiah, S. Sahdev, E.M. Shajil, T.K. Taneja, M. Mohan, M. Athar, N.K. Sah, M. Krishnaveni, Host-pathogen interactions during apoptosis, J. Biosci. 28 (2003) 349–358, https://doi.org/10.1007/BF02970153.

[48] H. Miyake, I. Hara, S. Kamidono, M. Gleave, H. Eto, Resistance to cytotoxic chemotherapy-induced apoptosis in human prostate cancer cells is associated with intracellular clusterin expression, Oncol. Rep. (2003) 469–473, https://doi.org/10.3892/or.10.2.469.

[49] I.P. Trougakos, A. So, B. Jansen, M.E. Gleave, E.S. Gonos, Silencing expression of the clusterin/apolipoprotein J gene in human cancer cells using small interfering RNA induces spontaneous apoptosis, reduced growth ability, and cell sensitization to genotoxic and oxidative stress, Cancer Res. 64 (2004) 1834–1842, https://doi.org/10.1158/0008-5472.CAN-03-2664.

[50] K.J. Joo, Role of clusterin and tumor necrosis factor receptors on the apoptosis of prostate cancer cells, Korean J. Androl. 29 (2011) 43, https://doi.org/10.5534/kja.2011.29.1.43.

[51] C.H. Coyle, L.J. Martinez, M.C. Coleman, D.R. Spitz, N.L. Weintraub, K.N. Kader, Mechanisms of H2O2-induced oxidative stress in endothelial cells, Free Radic. Biol.

Med. 40 (2006) 2206–2213, https://doi.org/10.1016/j.freeradbiomed.2006.02.017.
[52] H. Babich, M.R. Palace, A. Stern, Oxidative stress in fish cells:In vitro studies, Arch. Environ. Contam. Toxicol. 24 (1993) 173–178, https://doi.org/10.1007/BF01141344.
[53] D. Plesca, S. Mazumder, A. Almasan, Chapter 6 DNA damage response and apoptosis, in: Methods in Enzymology, Elsevier, 2008, pp. 107–122, https://doi.org/10.1016/S0076-6879(08)01606-6.
[54] V. Savković, H. Gantzer, U. Reiser, L. Selig, S. Gaiser, U. Sack, G. Klöppel, J. Mössner, V. Keim, F. Horn, H. Bödeker, Clusterin is protective in pancreatitis through anti-apoptotic and anti-inflammatory properties, Biochem. Biophys. Res. Commun. 356 (2007) 431–437, https://doi.org/10.1016/j.bbrc.2007.02.148.
[55] M.K. Ranney, I.S.A. Ahmed, K.R. Potts, R.J. Craven, Multiple pathways regulating the anti-apoptotic protein clusterin in breast cancer, in: Biochimica et Biophysica Acta (BBA) - Molecular Basis of Disease. 1772, 2007, pp. 1103–1111, https://doi.org/10.1016/j.bbadis.2007.06.004.
[56] N. Liang, S. Li, Y. Liang, Y. Ma, S. Tang, S. Ye, F. Xiao, Clusterin inhibits Cr(VI)-induced apoptosis via enhancing mitochondrial biogenesis through AKT-associated STAT3 activation in L02 hepatocytes, Ecotoxicol. Environ. Saf. 221 (2021), 112447, https://doi.org/10.1016/j.ecoenv.2021.112447.
[57] M.Y. Patel, K. Stovall, J.L. Franklin, The intrinsic apoptotic pathway lies upstream of oxidative stress in multiple organs, Free Radic. Biol. Med. 158 (2020) 13–19, https://doi.org/10.1016/j.freeradbiomed.2020.05.025.
[58] P. Li, D. Nijhawan, I. Budihardjo, S.M. Srinivasula, M. Ahmad, E.S. Alnemri, X. Wang, Cytochrome c and dATP-dependent formation of apaf-1/caspase-9 complex initiates an apoptotic protease cascade, Cell 91 (1997) 479–489, https://doi.org/10.1016/S0092-8674(00)80434-1.